Physics Letters A 378 (2014) 2989–2994

Contents lists available at ScienceDirect

Physics Letters A

www.elsevier.com/locate/pla

Theoretical study on Si-doped hexagonal boron nitride (*h*-BN) sheet: Electronic, magnetic properties, and reactivity

Yue-jie Liu *, Bo Gao, Duo Xu, Hong-mei Wang, Jing-xiang Zhao *

Key Laboratory for Photonic and Electronic Bandgap Materials, Ministry of Education, Harbin Normal University, Harbin, 150025, China

ARTICLE INFO

Article history:
Received 3 May 2014
Received in revised form 10 July 2014
Accepted 29 July 2014
Available online 26 August 2014
Communicated by V.A. Markel

Keywords:
h-BN sheet
Silicon-doped
Physical properties
Reactivity
DFT

ABSTRACT

The properties and reactivity of Si-doped hexagonal boron nitride (*h*-BN) sheets were studied using density functional theory (DFT) methods. We find that Si impurity is more likely to substitute the boron site (Si_B) due to the low formation energy. Si-doping severely deforms *h*-BN sheet, resulting in the local curvature changes of *h*-BN sheet. Moreover, Si-doping introduces two spin localized states within the band gap of *h*-BN sheet, thus rendering the two doped systems exhibit acceptor properties. The band gap of *h*-BN sheet is reduced from ∼4.70 eV to 1.24 (for Si_B) and 0.84 eV (for Si_N), respectively. In addition, Si-doped one exhibits higher activity than pristine one, endowing them wider application potential.

1. Introduction

Since the discovery of graphene in 2004 [1], extensive research has been conducted on novel analogous two-dimensional structures, such as hexagonal boron nitride (*h*-BN) sheet [2,3], which has been successfully synthesized in experiment [4–17]. Unlike graphene, the pristine *h*-BN sheet is intrinsically an insulator or a wide-band gap semiconductor, which is not ideal for electronic applications. Therefore, the modification of its properties through chemical functionalization is very important for specific application and many significant efforts have been made [18–33]. For example, the attachment of H [18], F [18,19], O [20], OH [21], CHO [22], NH_x [23], or organic molecules [24,25] to *h*-BN sheet can effectively modulate its electronic properties.

Alternatively, the substituted doping of foreign atoms to *h*-BN sheet is shown to be also effective to modify its electronic properties and has attracted a great deal of interest [34–38]. Currently, the most common dopant of *h*-BN sheet is carbon (C) [34], which is the neighbor of boron (B) and nitrogen (N) atoms in the periodic table. The synthesized C-doping of *h*-BN sheet [34,35] not only modifies its electronic structures, but also endows it with some new properties [34–36]. For example, Golberg et al. experimentally reported that the C-substitution can transform BN graphene from an electrical insulator to a conductor [34]. Tang and co-workers demonstrated that the doping of carbon chain makes *h*-BN sheet of ferromagnetic nature [36].

On the other hand, the doping of silicon (Si), which belongs to the same group as C, group IV, but strongly prefers sp^3-like bonding, is shown to influence the electronic and structural properties of graphene [39–41]. Theoretically, it was predicted that the large outward displacement of the Si atom and its nearest-neighbor C atoms may impose changes in the physical properties. For example, our previous studies have found that Si-doped graphene exhibits superior catalytic performance in CO oxidation [39] and NO reduction reactions [42]. Recently, Si-doped boron nitride nanotubes (BNNTs) have been synthesized via thermal chemical vapor deposition [43]. For the Si-doped BNNTs, the first-principle calculations showed that the formation energy of the incorporation of a Si atom into a B site of the single-walled nanotubes is low [43]. Meanwhile, the band gap of BNNTs is greatly reduced due to Si-doping [43]. Inspired by well-established Si-doping of graphene and BNNTs, theoretical study on the properties and applications Si-doped *h*-BN sheet is highly desirable although there has been no experimental evidence for the synthesis of Si-doped *h*-BN sheet until now. Intuitively, Si-doped *h*-BN sheet can be achieved in experiment by adopting the same technique as BNNT [43].

In this paper, by the means of the density functional theory (DFT) methods, we explore the doping of silicon atom inside *h*-BN sheet at two possible substitution sites: a boron site (Si_B) and a nitrogen site (Si_N). The following questions would be mainly addressed: (1) how do the geometric, electronic, and magnetic structures of *h*-BN sheet change? (2) After Si-doping, is the chemical reactivity of *h*-BN sheet toward some common gas molecules (such as CO, O_2, NH_3, and NO) modified? Knowledge gained from this

---

* Corresponding authors.

http://dx.doi.org/10.1016/j.physleta.2014.07.053

study may not only lead to a better understanding of the physical properties of *h*-BN sheet, but also have practical implications for the development of novel *h*-BN sheet-based nanodevices, such as gas sensor, metal-free catalysts, and so on, thereby greatly widening its potential applications.

2. Calculation methods and models

Calculations were based on the spin-polarized density functional theory (DFT) using generalized gradient approximation (GGA) for exchange-correlation potential prescribed by Perdew, Burke and Ernzerhof (PBE) [44], implemented in DMol^3 package [45]. All-electrons calculations were employed with the double numerical basis sets plus polarization functional (DNP), which are comparable to the Gaussian 6-31G (d, p) basis set in size and quality. A (5×5) supercell with the periodic boundary conditions on the x–y plane was employed. The vacuum space was set with 20 Å in the z direction to avoid the interactions between periodic images. A $3 \times 3 \times 1$ mesh of k-points [46] and the global orbital cutoff of 4.6 Å were used. All structures were fully relaxed without any symmetry constraints. Convergence in energy, force, and displacement were set as 10^{-5} Ha, 0.002 Ha/Å, and 0.005 Å, respectively. Charge transfers and magnetic moment were calculated with the Hirshfeld charge analysis method [47]. The accuracy of our procedure was tested using pristine BN nanosheet: the optimized bond length of B–N is 1.45 Å, which is in good agreement with Zhou's report (1.446 Å) [48].

The formation energy [49,50] for Si-doping into the *h*-BN sheet was defined as: $E_F = (E_{t1} - E_{t2}) - (E_1 - E_2)$, where E_{t1} is the total energy of *h*-BN sheet with substitutional doping, E_{t2} is the total energy of *h*-BN sheet, E_1 is the energy of single free silicon atom, E_2 is the energy of single free boron or nitrogen atom. The adsorption energy of gas molecules on the pristine or Si-doped *h*-BN sheet was evaluated as: $E_{ads} = E_{total}$ (*h*-BN sheet + gas molecule) $-E_{total}$ (*h*-BN sheet) $-E_{total}$ (gas molecule), where E_{total} stands for the total energy of the studied systems in the brackets. A negative E_{ads} corresponds to a stable structure.

It should be pointed out that we also perform test-calculations to evaluate the accuracy of adopted models. As shown in Table S1 of the Supporting Information, the obtained geometrical parameters through (5×5), (6×6), (7×7) supercells are nearly same. Moreover, by examining the adopted k-points of the Si$_N$ configuration, we find the $3 \times 3 \times 1$ mesh of k-points is enough accurate the behavior of Si-doped *h*-BN sheet according to the convergence test.

3. Results and discussion

3.1. The effects of Si-doping on geometric, electronic, and magnetic properties of *h*-BN sheet

First, we study the effects of Si-doping on the geometrical structures of *h*-BN sheet. After fully structural optimizations for Si$_B$ and Si$_N$ defects in *h*-BN sheet, we find that Si-doping causes significantly large distortion in *h*-BN sheet. For the Si$_B$ defect as shown in Fig. 1a, the equivalent three Si–N bond lengths in doped *h*-BN sheet are 1.73 Å, which are much larger than the B–N sp^2 bonds (1.45 Å) of pristine *h*-BN sheet. Moreover, Si atom preserves sp^3 nature, and bonds with tetrahedral-like configurations, with the average N–Si–N bond angles of 106°. The increase in bond lengths combined with the difference in bond angles forces the Si atom to protrude outwardly from the *h*-BN sheet surface by ∼ 0.68 Å. Meanwhile, the positions of the nearest three N atoms are out of the sheet surface to different degrees. These structural changes of *h*-BN sheet mainly come from the corrugation induced by the presence of the Si atom. The calculated formation energy of forming Si$_B$ defect in *h*-BN sheet is about 4.80 eV. As shown in Fig. 1b, the structural changes of *h*-BN sheet due to the Si$_N$ defect are very similar to those of the Si$_B$ defect: (1) the Si–B bond length is 1.95 Å, while the B–Si–B bond angle is close to 96°; (2) Si atom is pulled away from the surface of *h*-BN sheet by ∼ 1.00 Å. However, the formation energy of the Si$_N$ defect is 10.22 eV, which is much larger than that of Si$_B$ defect. This indicates that the Si$_B$ defect is more likely to present than Si$_N$ one.

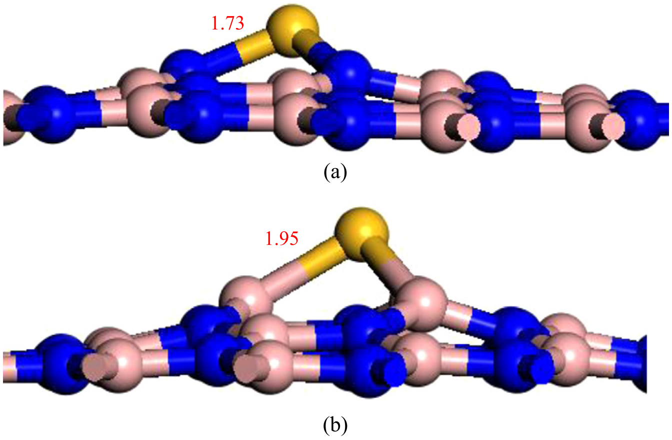

(a)

(b)

Fig. 1. The optimized structures of (a) Si$_B$ and (b) Si$_N$ defects in *h*-BN sheet. The unit of bond length is Å.

Moreover, there is about 0.36 (for Si$_B$ defect) or 0.09*e* (for Si$_N$ defect) charge transfer from Si to *h*-BN sheet, indicating that all types of vacancies in *h*-BN sheet are acceptors for Si adsorption, which is different from those of Au adsorption: *h*-BN sheets with B and N vacancies are shown to play a role of electron acceptors and donors for the adsorbed Au atom [51]. This difference may correlate with their electronegativity and Si exhibits stronger electron-donating capability than Au. The magnetic moment of the whole system is 1.00μ_B, which mainly originates from the contributions of Si impurity as shown in Fig. 2a and b. The charge transfer can also be verified by the difference of electronic densities of Si-doped BN sheet, as shown in Fig. 2c and d, where the red and blue regions represent the areas of electron accumulation and loss, respectively. Obviously, different electron affinities of Si and B or N change the electron distribution of the Si-doped *h*-BN sheet system. However, the whole *h*-BN sheet structure remains covalent in nature due to the electrons are mainly located within the bonds rather than heavily centered on the B or N atoms.

To gain deeper insights into the electronic structure of the two Si-doped *h*-BN sheets, we further calculated their band structures and density of states (DOS). Compared to the band structure of the perfect *h*-BN sheet (Fig. 3a), the Si$_B$ and Si$_N$ defects introduce two spin states within the band gap of *h*-BN sheet as shown in Fig. 3b and c, which gives rise to an unpaired spin (down) acceptor state (labeled as α and β in Fig. 3b and c, respectively) within the band gap of *h*-BN sheet. This leads to the reduction of the band gap from 4.71 eV of pristine *h*-BN sheet to 1.24 (Si$_B$ defect) and 0.84 eV (Si$_N$ defect), respectively, indicating a semiconducting nature. With the aim of investigating the spatial localization of the unpaired spin state, we analyzed the charge density for the lowest unoccupied molecular orbital (LUMO). Fig. 3d and e shows the charge density plot of the LUMO when the Si$_B$ and Si$_N$ defects are present in the *h*-BN sheet. It is found that for both *h*-BN sheets we studied, the main contribution for the LUMO comes from the Si atom, with small contributions coming from the nearest neighbors N and B atoms. Owing to the formation of three N–Si or B–Si bonds and charge transfer from Si-atom to *h*-BN sheet, the Si-3s, Si-3p, and B-, N-2p orbitals are partially filled, and strong hybridization between 3p states of Si-atom and 2p states of B- or N-atoms of *h*-BN